INTERNATIONAL JOURNAL FOR NUMERICAL METHODS IN FLUIDS, VOL. 22, 11–27 (1996)

FINITE ELEMENT ANALYSIS OF ANISOTROPIC FLUID SUSPENSIONS

G. F. CAREY, T. DAVID HU AND R. McLAY

Department of Aerospace Engineering and Engineering Mechanics, University of Texas at Austin, Austin, TX 78712, U.S.A.

SUMMARY

The orientation tensor **L** is introduced to construct a modified Leslie–Ericksen model for the viscous, incompressible flow of anisotropic suspensions (including electric field effects). This is then utilized to develop a weak variational formulation and finite element scheme for computing the flow and orientation fields. Numerical results are presented for exploratory test problems.

KEY WORDS: finite elements; liquid crystal; nematic; anisotropic; electrorheological

1. INTRODUCTION

The non-Newtonian behaviour of fluid suspensions is a complex subject that is receiving increasing attention. For example, there are several open research questions in constitutive theory, mathematical modelling and numerical simulation that are of major interest.[1–3] In particular, an improved understanding of the underlying processes and modelling techniques is critical to the analysis and development of engineering systems that involve the flow of suspensions. Applications include blood flow in biomedical engineering, frac fluid suspensions for fracturing in oil and gas reservoir stimulation and flow of pastes and creams in the chemical engineering, pharmaceutical and food-processing industries. In certain cases such as ferrofluids and electrorheological fluids the orientation of the suspension particles and flow also depends on applied exterior fields. For example, in electrorheological fluids the microstructure of the fluid aligns with the applied field gradient, which implies that the fluid properties (apparent viscosity) change on application of an electric field and depend on the local field strength.[4,5]

Experimental measurements have been made on a variety of fluid suspensions and these studies have led to the development of empirical formulas describing certain simple suspensions.[6] These results are to some extent experimentally incomplete. For instance, the standard simple shear flow experiment is not adequate to describe the behaviour of such fluids in a non-simple shear situation. Some of our recent work has been directed to experimental studies of dilute fluid suspension flow using nuclear magnetic resonance (NMR) imaging.[7]

Existing theoretical models are primarily designed for dilute to semidilute suspensions of monodispersed rigid spheres where particle–particle interactions are assumed small. Even in such cases where semiempirical theoretical models are available, mathematical modelling and numerical simulation for engineering applications remain formidable problems. The focus of the present investigation is the development of a mathematical formulation and finite element analysis based on a modified Leslie–Ericksen model for dilute anisotropic suspensions.[8]

CCC 0271–2091/96/010011–17

Received 18 November 1994
Revised 14 April 1995

The treatment proceeds as follows. In Section 2 we present the suspension fluid model investigated in the present work. This begins from the basic Leslie–Ericksen model which introduces an orientation vector field for the suspension. Then, using the approach of Doi, a tensor representation for orientation is introduced and this leads to a modified Leslie–Ericksen model. A variational form corresponding to this mathematical model is then constructed and an approximate formulation based on finite elements is developed in Section 3. Numerical experiments are presented in Section 4 for several basic benchmark flows and for a simple electrorheological flow model.

2. ANISOTROPIC SUSPENSION MODEL

2.1. Director field model

The Leslie–Ericksen (L–E) model was originally developed to study the anisotropic behaviour of nematic liquid crystals.[8] In addition to the usual primitive velocity–pressure $(\mathbf{u}, p)$ variables for viscous flows, the model introduces a new variable $\mathbf{n}$ called the 'director' to describe the orientation field for the anisotropic suspension. The director $\mathbf{n}$ at any point in the fluid is a unit vector oriented along the preferred direction (anisotropic or optical axis) of the fluid. In suspensions, $\mathbf{n}$ can represent the structure within a fluid due to either the microstructure of the suspended particles or the arrangement of particles relative to one another in the fluid.[1,9] Mathematically the L–E model involves including additional terms in the momentum conservation equations to describe the dependence of the elastic free energy W and stress on the director field $\mathbf{n}$.

More specifically, for conservation of linear momentum,[8]

$$\rho \frac{\mathrm{D}u_i}{\mathrm{D}t} = F_i - p_{,i} - \left(\frac{\partial W}{\partial n_{k,j}} n_{k,i} \right)_{,j} + \tau_{ij,j}, \tag{1}$$

where ρ is density, $\mathbf{u}$ is velocity, $\mathbf{F}$ is body force and $\boldsymbol{\tau}$ is an extra stress tensor. $\mathrm{D}/\mathrm{D}t$ denotes the material time derivative and standard indicial notation is implied. The effect of the suspension director field $\mathbf{n}$ enters in the last two terms of (1) involving the elastic free energy W and extra stress tensor $\boldsymbol{\tau}$ respectively. An additional normalization condition

$$\mathbf{n}\cdot\mathbf{n} = 1 \tag{2}$$

enters as a constraint on the director $\mathbf{n}$.

The elastic free energy W can be expressed as

$$W = \tfrac{1}{2}[K_1(\nabla\cdot\mathbf{n})^2 + K_2(\mathbf{n}\cdot\nabla\times\mathbf{n})^2 + K_3(\mathbf{n}\times\nabla\times\mathbf{n})^2], \tag{3}$$

where K_i are elastic constants. The extra stress tensor $\boldsymbol{\tau}$ has the form

$$\boldsymbol{\tau} = \alpha_1(\mathbf{n}\cdot\mathbf{D}\cdot\mathbf{n})\mathbf{n}\mathbf{n} + \alpha_2\mathbf{N}\mathbf{n} + \alpha_3\mathbf{n}\mathbf{N} + \alpha_4\mathbf{D} + \alpha_5(\mathbf{D}\cdot\mathbf{n})\mathbf{n} + \alpha_6\mathbf{n}(\mathbf{D}\cdot\mathbf{n}), \tag{4}$$

where α_i are termed Leslie viscosities and

$$\mathbf{N} = \frac{\mathrm{D}\mathbf{n}}{\mathrm{D}t} - \boldsymbol{\Omega}\cdot\mathbf{n}, \tag{5}$$

with $\boldsymbol{\Omega}$ the vorticity tensor.

Similarly, for conservation of angular momentum,

$$\sigma \frac{\mathrm{D}^2 n_i}{\mathrm{D}t^2} = G_i + \gamma n_i - \frac{\partial W}{\partial n_i} + \left(\frac{\partial W}{\partial n_{i,j}} \right)_{,j} + \tilde{g}_i, \tag{6}$$

where σ is an inertia constant (of rotation) and γ is the director tension (from the normalization constraint on $\mathbf{n}$). The additional vector fields $\mathbf{G}$ and $\tilde{\mathbf{g}}$ in (6) include the effect of an imposed electric field $\mathbf{E}$ and can be expressed as

$$\mathbf{G} = m\mathbf{E} = c[m^* + \Delta\alpha(\mathbf{E}\cdot\mathbf{n})]\mathbf{E}, \tag{7}$$

$$\tilde{\mathbf{g}} = -\gamma_1\mathbf{N} - \gamma_2(\mathbf{D}\cdot\mathbf{n}), \tag{8}$$

where $\mathbf{G}$ is the director body force and $\tilde{\mathbf{g}}$ characterizes the force arising from the difference in angular velocity between the director and the background fluid. Here m is the electric dipole moment associated with the field $\mathbf{E}$, m^* is the permanent dipole moment per unit volume, $\mathbf{D}$ is the rate-of-deformation tensor, $\mathbf{N}$ describes the rotation of the director with respect to the background fluid, c is the particle concentration and $\Delta\alpha = \alpha_{\|} - \alpha_{\perp}$, with $\alpha_{\|}$ and $\alpha_{\perp}$ the parallel and perpendicular polarities respectively. The coeficients γ_1 and γ_2 are defined in terms of the Leslie viscosities $\{\alpha_i\}$ by $\gamma_1 = \alpha_3 - \alpha_2$ and $\gamma_2 = \alpha_2 + \alpha_3 = \alpha_6 - \alpha_5$, where $\gamma_1 > 0$ and $\gamma_2 < 0$ usually apply (Reference 10, p. 231).

The conservation-of-mass equation

$$u_{i,i} = 0 \tag{9}$$

completes the governing system of partial differential equations (1), (6) and (9) for $\mathbf{u}$, p, $\mathbf{n}$ and γ.

Note that in the absence of an electric or magnetic field, $\mathbf{n}$ and $-\mathbf{n}$ are physically indistinguishable. This is not the case in the presence of an external field except when the particles have only induced dipoles ($m^* = 0$). In the present work we consider the typical case where the particles have negligible permanent dipole and the induced dipole is proportional to the local field.

On non-dimensionalizing the governing equations and considering the high-viscosity limit,[11] an explicit relationship for $\mathbf{N}(\mathbf{n})$ can be developed from (5) and (6). The angular momentum equation (6) then reduces to

$$\mathbf{G} + \gamma\mathbf{n} - \gamma_1\mathbf{N} - \gamma_2(\mathbf{D}\cdot\mathbf{n}) = 0. \tag{10}$$

Taking the dot product of (10) with $\mathbf{n}$, applying the normalization condition and simplifying gives

$$\gamma = \gamma_2(\mathbf{n}\cdot\mathbf{D}\cdot\mathbf{n}) - (\mathbf{G}\cdot\mathbf{n}). \tag{11}$$

Substituting in (10) and using (7), we obtain

$$\mathbf{N} = -\frac{\gamma_2}{\gamma_1}[(\mathbf{I} - \mathbf{nn})\cdot(\mathbf{D}\cdot\mathbf{n})] + \frac{c\Delta\alpha}{\gamma_1}(\mathbf{E}\cdot\mathbf{n})[(\mathbf{I} - \mathbf{nn})\cdot\mathbf{E}] + \frac{cm^*}{\gamma_1}[(\mathbf{I} - \mathbf{nn})\cdot\mathbf{E}], \tag{12}$$

where $\mathbf{I}$ is the identity (isotropic) tensor and $\mathbf{I} - \mathbf{nn}$ is the identity tensor on the spherical surface where the direction $\mathbf{n}$ resides.

Now, using this relationship for $\mathbf{N}(\mathbf{n})$ in (5), we can construct a reduced system with the evolution of the director field described by

$$\frac{\mathrm{D}\mathbf{n}}{\mathrm{D}t} = \boldsymbol{\Omega}\cdot\mathbf{n} + \lambda_1[(\mathbf{I} - \mathbf{nn})\cdot(\mathbf{D}\cdot\mathbf{n})] + \lambda_2(\mathbf{E}\cdot\mathbf{n})[(\mathbf{I} - \mathbf{nn})\cdot\mathbf{E}] + \lambda_3[(\mathbf{I} - \mathbf{nn})\cdot\mathbf{E}], \tag{13}$$

where

$$\lambda_1 = -\frac{\gamma_2}{\gamma_1} = \frac{\alpha_2 + \alpha_3}{\alpha_2 - \alpha_3} = \frac{1 + \alpha_3/\alpha_2}{1 - \alpha_3/\alpha_2}, \qquad \lambda_2 = \frac{c\Delta\alpha}{\gamma_1}, \qquad \lambda_3 = \frac{cm^*}{\gamma_1}$$

and for most suspensions $\alpha_2 < 0$, $\alpha_3 < 0$ with $\alpha_3 \approx 0$.[10]

Substituting also for **N** in (4), the extra stress tensor becomes

$$\boldsymbol{\tau} = 2\mu\mathbf{D} + [\mu_2(\mathbf{n}\cdot\mathbf{D}\cdot\mathbf{n}) + \mu_4(\mathbf{E}\cdot\mathbf{n})]\mathbf{nn} + 2\mu_3[\mathbf{n}(\mathbf{D}\cdot\mathbf{n}) + (\mathbf{D}\cdot\mathbf{n})\mathbf{n}] + \mu_5\mathbf{En} + \mu_6\mathbf{nE}, \tag{14}$$

where we have also regrouped terms and redefined the coefficients in a more standard form as

$$\mu = \tfrac{1}{2}\alpha_4, \qquad \mu_2 = \alpha_1 - \lambda_1(\alpha_2 + \alpha_3),$$
$$2\mu_3 = \alpha_5 + \alpha_2\lambda_1 = \alpha_6 + \alpha_3\lambda_1, \qquad \mu_4 = \lambda_1 m,$$
$$\mu_5 = \alpha_2[\lambda_2(\mathbf{E}\cdot\mathbf{n}) + \lambda_3], \qquad \mu_6 = \alpha_3[\lambda_2(\mathbf{E}\cdot\mathbf{n}) + \lambda_3].$$

The formulation can be modified[2] to treat a Bingham fluid by including an elastic yield stress G_1 (Reference 12, p. 308) so that the constitutive relation becomes

$$\boldsymbol{\tau} = 2\mu\mathbf{D} + [G_1 + \mu_2(\mathbf{n}\cdot\mathbf{D}\cdot\mathbf{n}) + \mu_4(\mathbf{E}\cdot\mathbf{n})]\mathbf{nn} + 2\mu_3[\mathbf{n}(\mathbf{D}\cdot\mathbf{n}) + (\mathbf{D}\cdot\mathbf{n})\mathbf{n}] + \mu_5\mathbf{En} + \mu_6\mathbf{nE}. \tag{15}$$

A finite element scheme on a discretization of the flow domain was developed for the above formulation, but numerical difficulties and numerical instabilities were encountered both in normalizing **n** and, more particularly, because **n** and $-\mathbf{n}$ are physically indistinguishable in the absence of an applied external field. This latter difficulty necessitates the development of a modified formulation. Consequently, we now develop a tensor extension of the previous model using an approach based on that of Doi[13] for nematic liquid crystals.

2.2. Tensor field model

The basic approach is to reformulate the equations in terms of the symmetric tensor $\mathbf{L} = \mathbf{nn}$ rather than explicitly in terms of the director vector **n**. Clearly **nn** and $(-\mathbf{n})(-\mathbf{n})$ are indistinguishable and **L** has eigenvalues $\sigma_1 = 1$ and $\sigma_2 = 0$. The eigenvector corresponding to the major eigenvalue $\sigma_1 = 1$ is simply **n**. To derive the transport equation for the tensor **L**, first take the tensor product of the director equation (13) with **n** to obtain

$$\left(\frac{\mathrm{D}\mathbf{n}}{\mathrm{D}t}\right)\mathbf{n} = \boldsymbol{\Omega}\cdot\mathbf{nn} + \lambda_1[\mathbf{D}\cdot\mathbf{nn} - (\mathbf{n}\cdot\mathbf{D}\cdot\mathbf{n})\mathbf{nn}] + \lambda_2[\mathbf{EE}\cdot\mathbf{nn} - (\mathbf{E}\cdot\mathbf{n})^2\mathbf{nn}] + \lambda_3[\mathbf{En} - (\mathbf{E}\cdot\mathbf{n})\mathbf{nn}] \tag{16}$$

and similarly

$$\mathbf{n}\left(\frac{\mathrm{D}\mathbf{n}}{\mathrm{D}t}\right) = \mathbf{n}(\boldsymbol{\Omega}\cdot\mathbf{n}) + \lambda_1[\mathbf{n}(\mathbf{D}\cdot\mathbf{n}) - (\mathbf{n}\cdot\mathbf{D}\cdot\mathbf{n})\mathbf{nn}] + \lambda_2[\mathbf{nn}\cdot\mathbf{EE} - (\mathbf{E}\cdot\mathbf{n})^2\mathbf{nn}] + \lambda_3[\mathbf{nE} - (\mathbf{E}\cdot\mathbf{n})\mathbf{nn}]. \tag{17}$$

Adding these equations and setting $\lambda_3 = 0$ for particles with negligible permanent dipoles, the evolution equation for the director tensor **L** is

$$\frac{\mathrm{D}\mathbf{L}}{\mathrm{D}t} = \boldsymbol{\Omega}\cdot\mathbf{L} - \mathbf{L}\cdot\boldsymbol{\Omega} + \lambda_1[\mathbf{D}\cdot\mathbf{L} + \mathbf{L}\cdot\mathbf{D} - 2(\mathbf{D}:\mathbf{L})\mathbf{L}] + \lambda_2[\mathbf{EE}\cdot\mathbf{L} + \mathbf{L}\cdot\mathbf{EE} - 2(\mathbf{EE}:\mathbf{L})\mathbf{L}], \tag{18}$$

where $\mathbf{D}:\mathbf{L} = D_{ij}L_{ij}$ and $\mathbf{EE}:\mathbf{L} = E_iE_jL_{ij}$. As indicated previously, the actual director field **n** can be recovered as the principal eigenvector of **L**. It is sometimes convenient to combine the last two terms in (18) to $\lambda_1[\mathbf{D}^*\cdot\mathbf{L} + \mathbf{L}\cdot\mathbf{D}^* - 2(\mathbf{D}^*:\mathbf{L})\mathbf{L}]$, where $\mathbf{D}^* = \mathbf{D} + (\lambda_2/\lambda_1)\mathbf{EE}$, so that the effect of the electric field can be interpreted through an additional stretching in the modified rate-of-strain tensor $\mathbf{D}^*$.

The stress tensor in (15) can be expressed similarly in terms of **L** as (see Appendix I)

$$\boldsymbol{\tau} = 2\mu\mathbf{D} + [G_1 + \mu_2(\mathbf{L}:\mathbf{D})]\mathbf{L} + 2\mu_3(\mathbf{D}\cdot\mathbf{L} + \mathbf{L}\cdot\mathbf{D}) + \lambda_2\gamma_1[(\mathbf{L}:\mathbf{EE})\mathbf{L} - \mathbf{EE}\cdot\mathbf{L}], \tag{19}$$

where we have again taken $\lambda_3 = 0$.

Remarks. It is straightforward to demonstrate that in the absence of an electric field and for the choice $\lambda_1 = 1$ the evolution equation (18) for $\mathbf{L}$ reduces to a form identical with Doi's molecular model for nematic liquid crystals at the high-viscosity limit. Note also that (18) can be interpreted as an evolution equation for each of the unknown components in the symmetric tensor $\mathbf{L}$.

3. NUMERICAL FORMULATION

3.1. *Weak formulation*

A weak integral formulation of the problem can be obtained by projection with an appropriate class of test functions. For simplicity of exposition let us begin by considering the governing equation (18) for the orientation tensor $\mathbf{L}$ in the absence of any applied electric field ($\mathbf{E} = \mathbf{0}$). Taking the integral projection with the test vector field $\mathbf{w}$, we have: find $\mathbf{L} \in T$, where T is the space of admissible solution components for $\mathbf{L}$, such that

$$\int_\Omega \left(\frac{\partial \mathbf{L}}{\partial t} + \mathbf{u}\cdot\nabla\mathbf{L}\right)\cdot\mathbf{w}\,dx = \int_\Omega (\boldsymbol{\Omega}\cdot\mathbf{L} - \mathbf{L}\cdot\boldsymbol{\Omega})\cdot\mathbf{w}\,dx + \lambda_1 \int_\Omega [\mathbf{D}\cdot\mathbf{L} + \mathbf{L}\cdot\mathbf{D} - 2(\mathbf{D} : \mathbf{L})\mathbf{L}]\cdot\mathbf{w}\,dx \tag{20}$$

holds for all admissible test fields $\mathbf{w}$.

A similar integral formulation can be obtained for the equations governing the conservation of linear momentum and mass. For the class of (high-viscosity) fluids of interest the inertia terms are negligible and can be omitted. Similarly, the viscous terms dominate the elastic terms which can also be neglected. Then, after integrating by parts in the weighted residual statement using the Gauss divergence theorem, the resulting variational statement is: find the velocity–pressure pair $(\mathbf{u}, p) \in V \times P$ satisfying the essential boundary conditions and such that

$$\rho \int_\Omega \frac{\partial \mathbf{u}}{\partial t}\cdot\mathbf{v}\,dx - \int_\Omega p\nabla\cdot\mathbf{v}\,dx + \int_\Omega \boldsymbol{\tau}:\nabla\mathbf{v}\,dx = \int_\Omega \mathbf{F}\cdot\mathbf{v}\,dx \tag{21}$$

for all admissible test velocities $\mathbf{v} \in V$, where the stress tensor in (19) simplifies for the case $\mathbf{E} = \mathbf{0}$, $G_1 = 0$ to

$$\boldsymbol{\tau} = 2\mu\mathbf{D} + \mu_2(\mathbf{L} : \mathbf{D})\mathbf{L} + 2\mu_3(\mathbf{D}\cdot\mathbf{L} + \mathbf{L}\cdot\mathbf{D}). \tag{22}$$

Finally, the weak integral condition for mass conservation is

$$\int_\Omega q\nabla\cdot\mathbf{u}\,dx = 0 \tag{23}$$

for all admissible pressure fields $q \in P$. Now (20)–(23) together with initial conditions comprise the weak integral statement of the problem. We recognize that (21) and (23) correspond to the weak statement for a viscous flow problem with the stress field defined by (22) and $\mathbf{L}$ satisfying (20). A semidiscrete Galerkin finite element scheme can now be developed based on this integral formulation.

3.2. *Finite element approximation*

First introduce a discretization of the domain as a partition of finite elements $\{\Omega_e\}$ and then define the approximation subspaces $T_h \subset T$, $V_h \subset V$ and $P_h \subset P$, where h denotes the mesh parameter. In the present work we use C^0 piecewise polynomial bases of Lagrange type and consider quadrilateral elements with biquadratic velocity and bilinear pressure fields. This choice of elements is known to satisfy the LBB (or inf-sup) stability condition for the finite element approximation of incompressible Navier–Stokes problems.[14] A bilinear basis is also employed for the components $(l_{ij})_h$ of the tensor $\mathbf{L}_h$. Since $\mathbf{L}$ is symmetric, only the entries l_{ij}, $j \geq i$, need be considered.

Substituting $\mathbf{L}_h$, $\mathbf{u}_h$, p_h for $\mathbf{L}$, $\mathbf{u}$, p in (20)–(23) and similarly $\mathbf{w}_h$, $\mathbf{v}_h$, q_h, for test functions $\mathbf{w}$, $\mathbf{u}$, q, the Galerkin finite element formulation is to find $\mathbf{L}_h$, $\mathbf{u}_h$, $p_h \in T_h \times V_h \times P_h$ approximating the essential boundary conditions and initial conditions and such that

$$\int_\Omega \left(\frac{\partial \mathbf{L}_h}{\partial t} + \mathbf{u}_h \cdot \nabla \mathbf{L}_h\right) \cdot \mathbf{w}_h \, dx - \int_\Omega (\boldsymbol{\Omega}_h \cdot \mathbf{L}_h - \mathbf{L}_h \cdot \boldsymbol{\Omega}_h) \cdot \mathbf{w}_h \, dx - \lambda_1 \int_\Omega [\mathbf{D}_h \cdot \mathbf{L}_h + \mathbf{L}_h \cdot \mathbf{D}_h - 2(\mathbf{D}_h : \mathbf{L}_h)\mathbf{L}_h] \cdot \mathbf{w}_h \, dx = 0, \tag{24}$$

$$\rho \int_\Omega \frac{\partial \mathbf{u}_h}{\partial t} \cdot \mathbf{v}_h \, dx - \int_\Omega p_h \nabla \cdot \mathbf{v}_h \, dx + \int_\Omega \boldsymbol{\tau}_h : \nabla \mathbf{v}_h \, dx = \int_\Omega \mathbf{F} \cdot \mathbf{v}_h \, dx, \tag{25}$$

$$\int_\Omega q_h \nabla \cdot \mathbf{u}_h \, dx = 0 \tag{26}$$

hold for all admissible test functions $\mathbf{w}_h$, $\mathbf{v}_h$, q_h and where we have written for convenience

$$\begin{aligned} &\mathbf{D}_h = \tfrac{1}{2}(\nabla \mathbf{u}_h + \nabla \mathbf{u}_h^{\mathrm{T}}), \qquad \boldsymbol{\Omega}_h = \tfrac{1}{2}(\nabla \mathbf{u}_h - \nabla \mathbf{u}_h^{\mathrm{T}}), \\ &\boldsymbol{\tau}_h = 2\mu \mathbf{D}_h + \mu_2 (\mathbf{L}_h : \mathbf{D}_h)\mathbf{L}_h + 2\mu_3 (\mathbf{D}_h \cdot \mathbf{L}_h + \mathbf{L}_h \cdot \mathbf{D}_h). \end{aligned} \tag{27}$$

The semidiscrete expansions for $\mathbf{L}_h$, $\mathbf{u}_h$, p_h have the form

$$(l_{ij})_h = \sum_{k=1}^{N_L} (l_{ij}(t))_k \Phi_k(\mathbf{x}), \qquad (u_i)_h = \sum_{j=1}^{N_v} (u_i(t))_j \chi_j(\mathbf{x}), \qquad p_h = \sum_{m=1}^{N_p} p_m(t) \Psi_m(\mathbf{x}), \tag{28}$$

where the nodal unknowns depend continuously on time t. Substituting the expansions (28) in (24)–(26) and similarly setting Φ_r, χ_s and Ψ_t for the corresponding components of the test functions, we obtain a semidiscrete system of ordinary differential equations for the nodal unknowns $\hat{\mathbf{L}}(t)$, $\mathbf{U}(t)$, $\mathbf{p}(t)$ of the form

$$\mathbf{M}_1 \frac{d\hat{\mathbf{L}}}{dt} + \mathbf{C}_1(\mathbf{U})\hat{\mathbf{L}} - \mathbf{Q}(\mathbf{U})\hat{\mathbf{L}} - \lambda_1 \mathbf{O}(\mathbf{U})\hat{\mathbf{L}} = \mathbf{0}, \tag{29}$$

$$\mathbf{M}_2 \frac{d\mathbf{U}}{dt} + \mathbf{C}_2(\mathbf{U})\mathbf{U} + \mathbf{B}\mathbf{p} + \mathbf{A}(\hat{\mathbf{L}})\mathbf{U} = \mathbf{0}, \tag{30}$$

$$\mathbf{B}^{\mathrm{T}}\mathbf{U} = \mathbf{0}, \tag{31}$$

where $\hat{\mathbf{L}}(t)$ denotes the global vector of components $l_{ij}(t)$, $j \geq i$, at the nodes of the discretization, $\mathbf{U}(t)$ denotes the usual global vector of velocity components and $\mathbf{p}(t)$ is the corresponding global vector of nodal pressures.

3.3. Time integration and sparse solution

The semidiscrete system (29)–(31) can be integrated using a variety of schemes. In the present work an implicit integration scheme is used, because the stiffness of the system may be quite large owing to the sensitivity of the orientation field to local changes in the velocity. Differencing (29) and (30) implicitly then leads to a large coupled non-linear system of algebraic equations to be solved at each time step. In fact, since the orientation field is strongly dependent on the local flow, but not *vice versa*, iterative decoupling of the system should provide a more efficient algorithm. Other integration schemes such as explicit methods and predictor–corrector strategies can also be constructed but are not considered here.

The non-linearity is represented by the dependence of the matrices $\mathbf{C}_1$, $\mathbf{Q}$, $\mathbf{O}$, $\mathbf{C}_2$ and $\mathbf{A}$ in (29) and (30) on the respective solution vectors. This can be conveniently treated by a successive approximation iteration or by Newton–Raphson iteration within each time step. The solution at the previous time step provides an appropriate starting iterate. In the successive approximation scheme for example, the resulting sparse system at iteration $s+1$ of time step $n+1$ reduces to

$$\mathbf{K}_1(\mathbf{U}_s^{n+1})\hat{\mathbf{L}}_{s+1}^{n+1} = \mathbf{H}_s^{n+1}, \tag{32}$$

$$\mathbf{K}_2(\mathbf{U}_s^{n+1},\ \hat{\mathbf{L}}_s^{n+1})\mathbf{U}_{s+1}^{n+1} + \mathbf{B}\mathbf{p}_{s+1}^{n+1} = \mathbf{C}_s^{n+1}, \tag{33}$$

$$\mathbf{B}^{\mathrm{T}}\mathbf{U}_{s+1}^{n+1} = \mathbf{0}. \tag{34}$$

Note that in this formulation the subsystem for $\hat{\mathbf{L}}$ decouples from the viscous flow equations. However, this scheme converges only linearly and the non-linear coupling is less strongly enforced within each iterative step. Newton's method leads to a fully coupled system, but convergence within a time-step may be better (Newton converges quadratically near a solution).

Some comments on the element calculations for the system matrices are warranted. First, the element integrals are evaluated using Gaussian quadrature. This implies that material properties μ, μ_2, μ_3 and field variables or derived quantities (such as $\boldsymbol{\Omega}_h$) must be supplied or interpolated at the Gauss points.

Let the non-linear system arising from implicit differencing of (29)–(31) be denoted $\mathbf{F}(\mathbf{z}) = \mathbf{0}$, where $\mathbf{z}$ is the full vector of nodal unknowns $\mathbf{z}_1 = \hat{\mathbf{L}}$, $\mathbf{z}_2 = \mathbf{U}$, $\mathbf{z}_3 = \mathbf{p}$. The familiar Newton iteration is then: given $\mathbf{z}_0$, for iterate $s = 1, 2, \ldots$ compute

$$\mathbf{z}_{s+1} = \mathbf{z}_s - \mathbf{J}_s^{-1}\mathbf{F}(\mathbf{z}_s) \tag{35}$$

or, equivalently, solve

$$\mathbf{J}_s\delta\mathbf{z} = -\mathbf{F}(\mathbf{z}_s), \tag{36}$$

where the Jacobian matrix $\mathbf{J}_s = \partial\mathbf{F}/\partial\mathbf{z}$ at $\mathbf{z} = \mathbf{z}_s$.

Let $\mathbf{f}_1$, $\mathbf{f}_2$, $\mathbf{f}_3$ denote the components of $\mathbf{F}$ associated with (29)–(31) respectively. At $t^* = t_m + \theta\Delta t$, $0 < \theta \leq 1$, the Jacobian entries for $\partial\mathbf{f}_i/\partial\mathbf{z}_1$ are

$$\begin{aligned} &\frac{\partial\mathbf{f}_1}{\partial\hat{\mathbf{L}}} = \mathbf{M}_1 + [\mathbf{C}_1(\mathbf{U}) + \mathbf{Q}(\mathbf{U}) - \lambda_1\mathbf{O}(\mathbf{U})]\theta\Delta t, \\ &\frac{\partial\mathbf{f}_2}{\partial\hat{\mathbf{L}}} = \left(\frac{\partial}{\partial\hat{\mathbf{L}}}\mathbf{A}(\hat{\mathbf{L}})\mathbf{U}\right)\theta\Delta t, \qquad \frac{\partial\mathbf{f}_3}{\partial\hat{\mathbf{L}}} = \mathbf{0}. \end{aligned} \tag{37}$$

Similarly, for $\partial\mathbf{f}_i/\partial\mathbf{z}_2$,

$$\begin{aligned} &\frac{\partial\mathbf{f}_1}{\partial\mathbf{U}} = \frac{\partial}{\partial\mathbf{U}}\{[\mathbf{C}_1(\mathbf{U}) - \mathbf{Q}(\mathbf{U}) - \lambda_1\mathbf{O}(\mathbf{U})]\hat{\mathbf{L}}\}\theta\Delta t, \\ &\frac{\partial\mathbf{f}_2}{\partial\mathbf{U}} = \mathbf{M}_2 + \left(\frac{\partial}{\partial\mathbf{U}}[\mathbf{C}_2(\mathbf{U})\mathbf{U}] + \mathbf{A}(\hat{\mathbf{L}})\right)\theta\Delta t, \qquad \frac{\partial\mathbf{f}_3}{\partial\mathbf{U}} = \mathbf{B}^{\mathrm{T}}. \end{aligned} \tag{38}$$

Finally, for $\partial\mathbf{f}_i/\partial\mathbf{z}_3$,

$$\frac{\partial\mathbf{f}_1}{\partial\mathbf{p}} = \mathbf{0} \qquad \frac{\partial\mathbf{f}_2}{\partial\mathbf{p}} = \theta\Delta t\mathbf{B}, \qquad \frac{\partial\mathbf{f}_3}{\partial\mathbf{p}} = \mathbf{0}. \tag{39}$$

Thus the Jacobian matrix is a 3×3 block matrix with entries in block columns 1–3 given by (37)–(39) respectively.

The Jacobian matrix for the system is accumulated from element contributions $\{\mathbf{j}_e = \partial \mathbf{f}^e / \partial \mathbf{z}^e\}$ for representative element e, where the element integrals for $\{\mathbf{j}_e\}$ are evaluated in the standard manner by Gaussian quadrature. This implies that in the element quadrature, solution values from the previous iterate are interpolated at the Gauss points. In particular, the approximate tensor components $(l_{ij})_h$ are interpolated at the Gauss points.

3.4. Electric field effects

In the preceding formulation we excluded electric field effects so that the main construction could be presented concisely. It is straightforward to generalize this treatment to include the effect of an electric field $\mathbf{E}$ which induces an electric dipole of moment m per unit volume. To do so, we first rewrite the transport equation for $\mathbf{L}$ in (18) as

$$\frac{\mathrm{D}\mathbf{L}}{\mathrm{D}t} = \mathbf{\Omega}\cdot\mathbf{L} - \mathbf{L}\cdot\mathbf{\Omega} + \lambda_1[\mathbf{D}^*\cdot\mathbf{L} + \mathbf{L}\cdot\mathbf{D}^* - 2(\mathbf{D}^*\colon \mathbf{L})\mathbf{L}], \tag{40}$$

where

$$\mathbf{D}^* = \mathbf{D} + \frac{\lambda_2}{\lambda_1}\mathbf{E}\mathbf{E} \tag{41}$$

is a modified rate-of-strain tensor. Hence inclusion of the electric field in the transport equation for $\mathbf{L}$ can be accomplished by simply introducing the modified rate-of-strain tensor $\mathbf{D}^*$ for $\mathbf{D}$. Similarly, the stress tensor $\boldsymbol{\tau}$ has the additional electric field contribution given in (19).

Given a specified field $\mathbf{E}$, the weak integral statement and Galerkin finite element formulation can be modified directly to incorporate the electric field contribution. More specifically, in the integral statement (24) for $\mathbf{L}$ we replace $\mathbf{D}_h$ by $\mathbf{D}_h^*$, the approximation to $\mathbf{D}^*$ in (41). Similarly, the relation for stress in (19) including the contributions from $\mathbf{E}$ now applies. The time integration procedure and Newton solution scheme follow as before.

In the numerical studies following, we consider the steady state case for an electrostatic field. Then $\mathbf{E} = \nabla\varphi$, where the electrostatic potential φ satisfies the Poisson equation

$$-\Delta\varphi = q/\varepsilon, \tag{42}$$

where q is the charge density and ε is the permittivity. The corresponding weak statement for this potential problem is: find $\varphi \in H^1$ satisfying the essential boundary conditions on φ and such that

$$\int_\Omega \nabla\varphi\cdot\nabla v\,\mathrm{d}x = \int_\Omega (q/\varepsilon)v\,\mathrm{d}x \tag{43}$$

holds for all $v \in H^1$, with $v = 0$ on that part of the boundary where φ is specified and where H^1 is the standard Hilbert space of admissible potentials. The finite element Galerkin statement follows similarly on replacing φ by φ_h and v by v_h in (43). This leads to a sparse symmetric positive system that is decoupled from the suspension flow equations and can be solved in advance to determine φ_h and thereby $\mathbf{E}_h = \nabla\varphi_h$. This fixed field can then be used in (41) and (19) to include the electric field effect on particle orientation and the suspension flow.

4. NUMERICAL STUDIES

We consider several fundamental test cases for steady two-dimensional flow of a suspension both in the absence and presence of an external electric field. Since the flow is assumed two-dimensional, it

follows that [15]

$$\mathbf{n}(\mathbf{D}\cdot\mathbf{n}) + (\mathbf{D}\cdot\mathbf{n})\mathbf{n} - \mathbf{D} = (\mathbf{n}\cdot\mathbf{D}\cdot\mathbf{n})\mathbf{I}, \tag{44}$$

which implies that the velocity and orientation fields depend only on the sum $\mu + \mu_3$. Hence varying μ and μ_3 such that $\mu + \mu_3$ remains constant will influence only the pressure field. Since the extra stress $\boldsymbol{\tau}$ is in general not traceless, we therefore define the modified hydrodynamic pressure

$$\hat{p} = p - tr(\boldsymbol{\tau})/3, \tag{45}$$

where $\hat{p}$ is the modified pressure, $\hat{p} = p - \rho\mathbf{g}\cdot\mathbf{r} + p_0$, with $\mathbf{g}$ the gravitational constant, $\mathbf{r}$ the position vector and p_0 a constant. Finally, the pair (μ, ρ) is chosen so that the Reynolds number is 10^{-4} and the viscosity scale is chosen to be the isotropic viscosity μ.

Case 1. Flow between parallel plates

Consider the steady flow of a suspension between two parallel plates. A fully developed flow is assumed at the inlet $x = 0$ and at the outlet $x = 1$. A 'no-slip' boundary condition is enforced at the lower wall $y = 0$. The horizontal symmetry line $y = 1$ is a 'slip line'. The pressure is determinable within an arbitrary constant and in the present calculations we specify this constant without loss of generality by setting the pressure to be zero at the centreline of the inlet ($x = 0, y = 1$).

An analytical solution can be derived for this problem in the absence of an electric field.[2] Therefore this provides an appropriate validation test. Assuming that the horizontal velocity component u is a function of y only, then the parabolic, fully developed profile satisfies the momentum and mass conservation equations. The equation for $\mathbf{L}$ is decoupled, and solving for the director angle β with $\mathbf{n} = (\cos\beta, \sin\beta)$, we obtain (see Appendix II)

$$\beta = \pm\tan^{-1}\left[\sqrt{\left(\frac{\lambda_1 - 1}{\lambda_1 + 1}\right)}\right]. \tag{46}$$

If $\lambda_1 < 1$, there is no steady state solution and the director $\mathbf{n}$ will 'tumble'. If $\lambda_1 \geq 1$, it can be shown that only the positive solution remains stable.

In the numerical experiment the orientation β of the directors at the inlet is specified by (46). The initial orientation of the directors elsewhere in the flow is chosen to coincide with the principal axis of stretching of the rate-of-strain tensor $\mathbf{D}$. Since the director transport equation is hyperbolic, no boundary condition orientation is specified at the outlet. The solution for the flow and orientation tensor is computed on a 5×5 mesh of square elements with biquadratic velocity, bilinear pressure and postprocessed bilinear director fields on each element. The system is integrated with time step $\Delta t = 1$ until the respective fields have essentially reached steady state at $t = 111$. The initial and final orientation fields are shown in Figures 1(a) and 1(b) and the velocity and pressure fields in Figure 1(c) and 1(d) respectively. The maximum nodal error in the director field compared with the exact solution in (46) is 5×10^{-4}. This occurs on the centreline $y = 1$ where the velocity gradient vanishes. (Since the velocity gradient vanishes on the centreline, the director can take any orientation on the centreline. That is, since the director elasticity has been neglected in the L–E model, the equilibrium orientation of the director at the centreline is not uniquely defined and can take any direction.)

The previous parallel plate flow problem is now considered with an applied electric field. The potential on the lower plate is unity and that on the symmetry plane is zero. The electrostatic potential equation is solved and the electric field computed at the Gauss points of each element. This is then used in the element calculations for the Jacobian matrix of the suspension flow equations. In the present work we assume that there are no orientation-dependent electrical properties within the fluid. The flow is driven by pressure drop, where the same normal stress (τ_{xx}) drop across the domain is

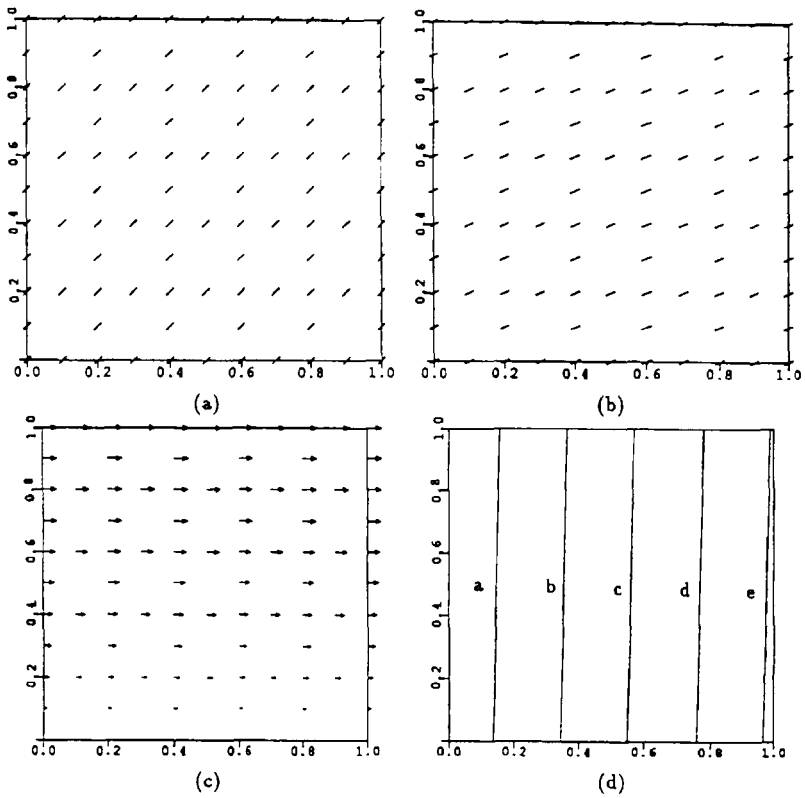

Figure 1. $G_1 = 0$, $\mu_2 = 0{\cdot}1$, $\mu_3 = -0{\cdot}05$, $\lambda_1 = 1{\cdot}5$: (a) initial director orientation; (b) director orientation at $t = 111$; (c) velocity profile at $t = 111$ with a maximum of 1·0; (d) pressure values $\hat{\gamma}$—a, $-0{\cdot}3$; b, $-0{\cdot}7$; c, $-1{\cdot}1$; d, $-1{\cdot}5$; e, $-1{\cdot}9$

specified as in the previous study. The initial orientation of the director is taken to be vertical throughout the suspension, including at the inlet. The applied electric field produces a local dipole effect that acts to orient and anchor the director, so we set $\lambda_1 = 1$ as explained in the discussion of the electric stress in Appendix I. In the present calculation we also set $\lambda_2 = 10$, which implies that the electric field effect will dominate the orientation pattern behaviour. That is, the electrical contribution to the director orientation is 10 times stronger than that due to the velocity gradient. Finally, we set $\lambda_3 = 0$, so that there is no permanent dipole in the director, and $\gamma_1 = 0{\cdot}2$, which implies that the electric field contribution to the stress tensor is approximately the same size as that due to the Newtonian viscosity. As expected, the electric field is essentially constant across the domain in this example. The evolved steady solutions for the orientation field and pressure distribution are shown in Figures 2(a) and 2(b) respectively and can be compared with the previous results in Figure 1. The effect of the applied field is to orient the director in the vertical direction as shown. However, in the vicinity of the bottom wall the velocity gradient is stronger and the orientation field still deviates slightly from the vertical. As expected, there is an increase in the effective viscosity due to the vertical orientation (Reference 16, p. 145) which makes the maximum velocity drop from 1·0 in Figure 1(c) to 0·883045. The velocity profile is essentially unchanged by the director re-orientation due to the applied electric field in this example.

Remarks. If elastic terms are included, the solutions are very different from those obtained with the high-viscosity approximation.[17,18] For instance, in the parallel plate flow problem leading to (46), the

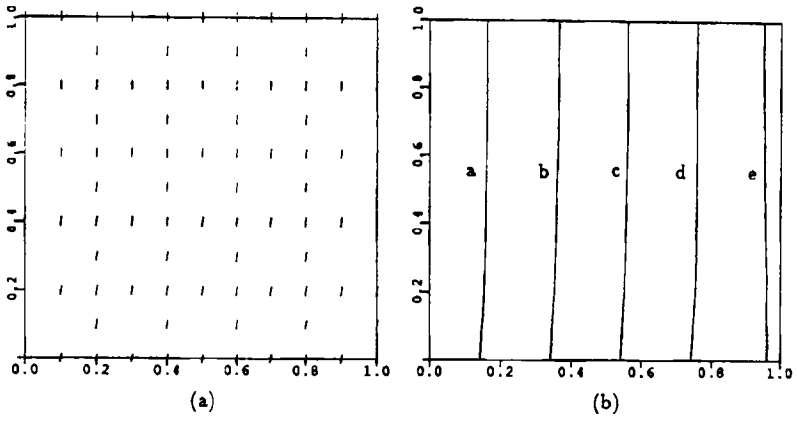

Figure 2. $G_1 = 0$, $\mu_2 = 0{\cdot}1$, $\mu_3 = -0{\cdot}05$, $\lambda_1 = 1{\cdot}0$, $\lambda_2 = 10$, $\lambda_3 = 0$, $\gamma_1 = 0{\cdot}2$: (a) director orientation at $t = 193$; (b) pressure values λ: a $= -0{\cdot}3$; b $= -0{\cdot}7$; c $= -1{\cdot}1$; d $= -1{\cdot}5$; e $= -1{\cdot}9$

director angle will no longer be a constant when elastic effects are included. In fact, for the parallel plate case the velocity and particle orientation are functions of y alone and the problem simplifies accordingly.[17] Other studies for $\lambda_1 < 1$ (where the director **n** 'tumbles') and with the elastic terms included have also been reported.[19,20]

Case 2. Channel with bump constriction

Next we consider the same class of channel flows with specified fully developed inlet and outlet velocity profiles, but in the presence of a smooth 'bump' constriction in the centre region. The symmetric lower half of the flow domain with its finite element mesh is shown in Figure 3. The first calculation was made in the absence of any electric field and for $\lambda_1 = 5{\cdot}0$. The velocity and pressure fields at steady state are shown in Figure 4. The normal stress drops from 0 to -27 across the domain. A sequence of director patterns at $t = 0{\cdot}0$, $0{\cdot}2$, $0{\cdot}7$ and essentially steady state ($t = 48$) is shown in Figure 5. To validate the computations, a finer 5×40 mesh was also used and no visible difference was observed. Hence we use the 4×25 mesh in the remainder of the study. The time step for these calculations was $\Delta t = 3 \times 10^{-5}$ s owing to the sensitivity of the orientation calculation. Note that the computed orientation field is not symmetric. In particular, following the bump constriction, the flow undergoes an extensional motion during the expansion region and the associated velocity gradient is such that the director tries to align with the vertical axis. This effect is evident in the figure. Also note that along the horizontal symmetry centreline the director orientation slope declines to zero as the bump is approached and then the director slope increases abruptly to a vertical orientation as the flow expansion region is encountered. The maximum velocity of 1·849 occurs at the centre of the constriction. Next the problem was recomputed with $\lambda_1 = 1{\cdot}5$. Although the velocity and pressure fields are essentially unchanged, there are some significant changes in the director field as shown in Figure 6. Since λ_1 is smaller, the 'anchoring' effect of the velocity gradients is diminished. Hence the director slope does not decrease as rapidly along the centrelines as in the case with $\lambda_1 = 5{\cdot}0$. Downstream on the centreline, the director has a tendency to align normal to the flow as in the previous case. However, the stretching effect due to the expansion is not sufficient to 'anchor' the orientation and the director field can deviate through either a clockwise or counterclockwise rotation as seen at various times in Figure 7.

Apparently there are two possible orientation solutions corresponding to positive or negative slopes respectively. The initial configuration and contraction flow favour the positive slope orientation, but

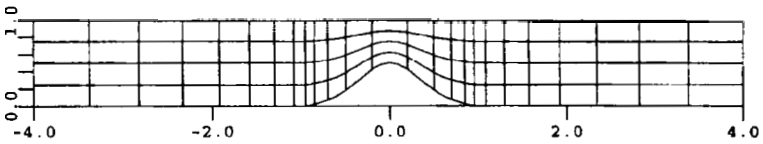

Figure 3. Mesh for parallel plates with constriction

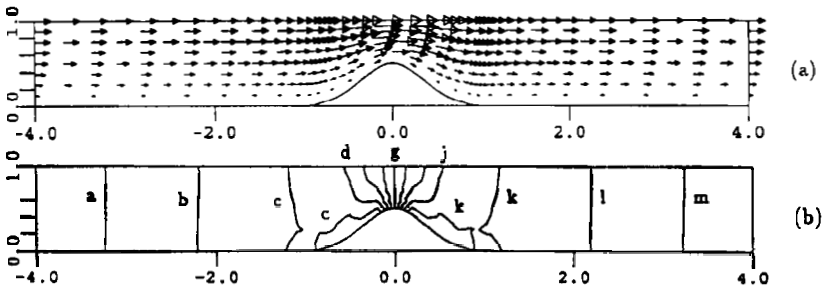

Figure 4. $G_1 = 0$, $\mu_2 = 0{\cdot}1$, $\mu_3 = -0{\cdot}05$, $\lambda_1 = 5{\cdot}0$: (a) velocity field at $t = 48$ with a maximum of 1·85; (b) pressure values λ: a = −1·5; b = −3·5; c = −5·5; d = −7·5; g = −13·5; j = −19·5; k = −21·5, −23·5; m = −25·5

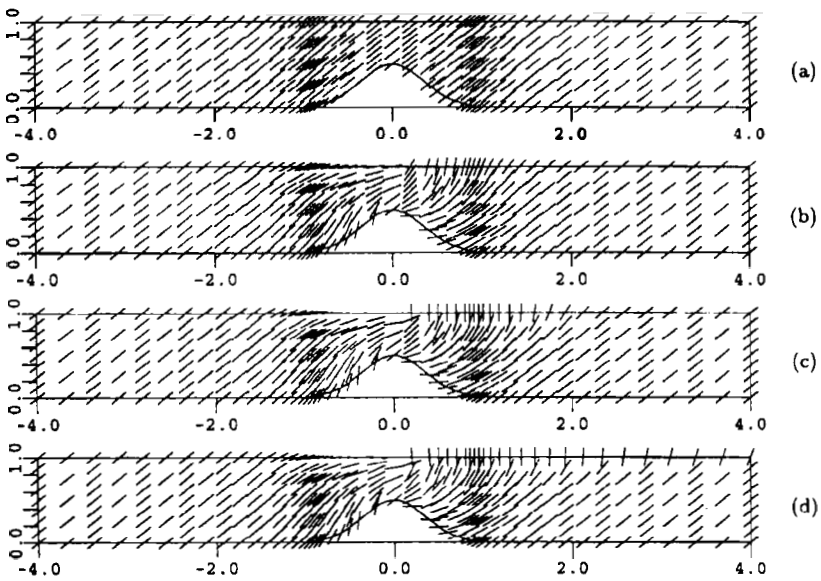

Figure 5. $G_1 = 0$, $\mu_2 = 0{\cdot}1$, $\mu_3 = -0{\cdot}05$, $\lambda_1 = 5{\cdot}0$: (a) initial director orientation; (b) director orientation at $t = 0{\cdot}2$; (c) at $t = 0{\cdot}7$; (d) at $t = 48$

along the centreline after the constriction the extensional stretching is such that either orientation may appear and the director orientation field can oscillate. This in turn will induce very small oscillations in the velocity and pressure fields.

Next we considered the sensitivity of the orientation field solution to different choices of viscosity coefficients $(\mu_2, \mu_3) = (1, -0{\cdot}5)$, $(2, -0{\cdot}5)$ and $(1, -1)$ at $\lambda_1 = 5{\cdot}0$, i.e. $\mu_2 + \mu_3 = 0{\cdot}5$, 1·5 and 0.

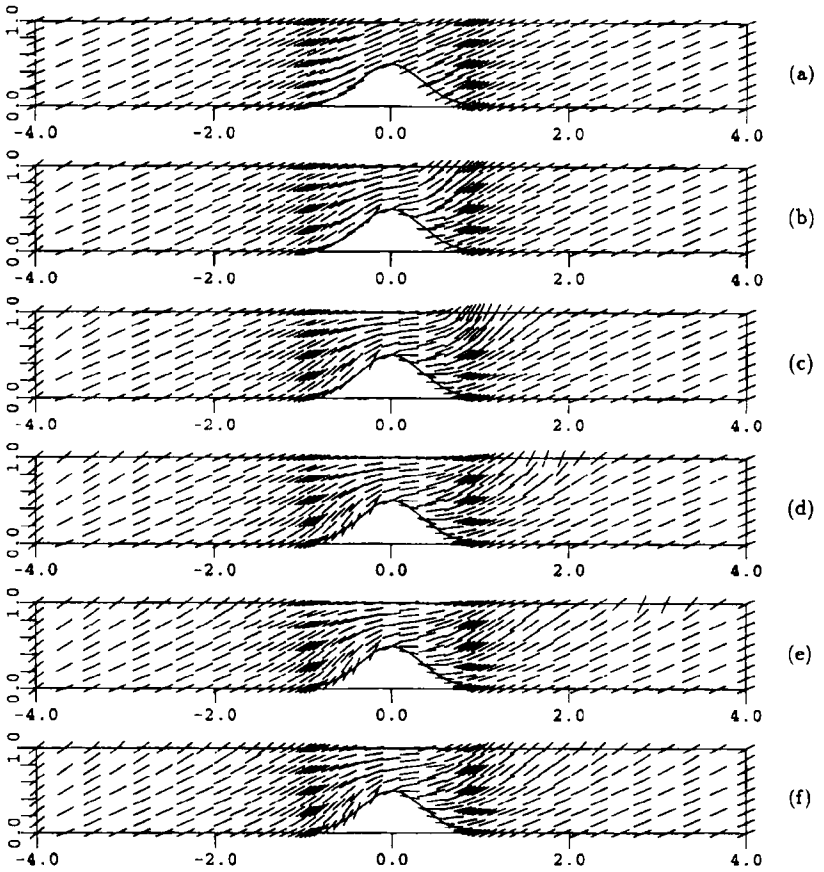

Figure 6. $G_1 = 0$, $\mu_2 = 0{\cdot}1$, $\mu_3 = -0{\cdot}05$, $\lambda_1 = 1{\cdot}5$: (a) initial director orientation; (b) director orientation at $t = 0{\cdot}26$; (c) at $t = 0{\cdot}69$; (d) at $t = 1{\cdot}45$; (e) at $t = 2{\cdot}67$; (f) at $t = 6{\cdot}19$

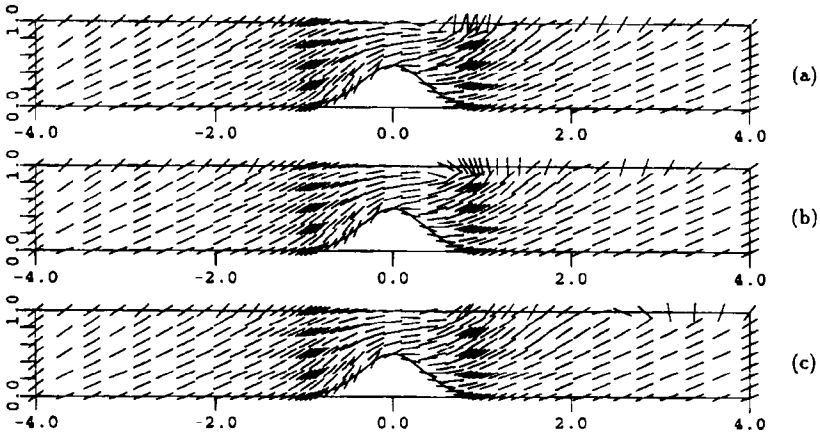

Figure 7. $G_1 = 0$, $\mu_2 = 0{\cdot}1$, $\mu_3 = -0{\cdot}05$, $\lambda_1 = 1{\cdot}5$: (a) director orientation at $t = 9{\cdot}82$; (b) at $t = 11{\cdot}92$; (c) at $t = 14{\cdot}34$

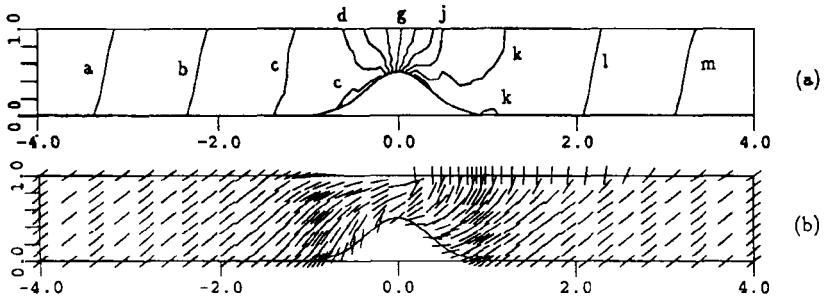

Figure 8. $G_1 = 0$, $\mu_2 = 1$, $\mu_3 = -0{\cdot}5$, $\lambda_1 = 5{\cdot}0$: (a) pressure values γ: a = −1·5; b = −3·5; c = −5·5; d = −7·5; g = −13·5; j = −19·5; k = −21·5; l = −23·5; m = −25·5—at $t = 1{\cdot}23$; (b) director orientation at $t = 1{\cdot}23$

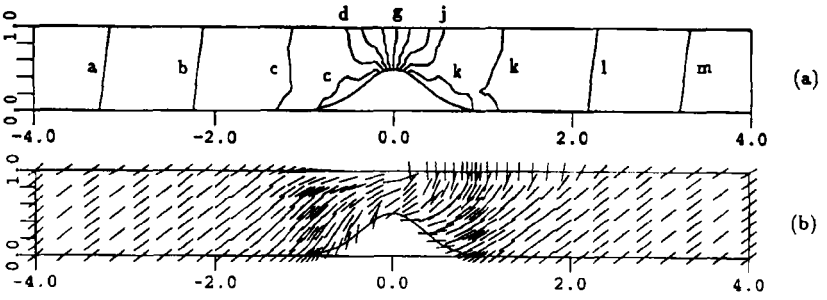

Figure 9. $G_1 = 0$, $\mu_2 = 2$, $\mu_3 = -0{\cdot}5$, $\lambda_1 = 5{\cdot}0$: (a) pressure values γ: a = −1·5; b = −3·5; c = −5·5; d = −7·5; g = −13·5; j = −19·5; k = −21·5; l = −23·5; m = −25·5—at $t = 1{\cdot}04$; (b) director orientation at $t = 1{\cdot}04$

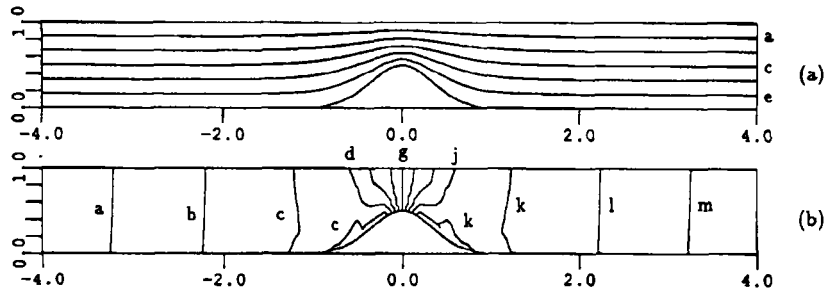

Figure 10. $G_1 = 0$, $\mu_2 = 0{\cdot}1$, $\mu_3 = -0{\cdot}05$, $\lambda_1 = 1{\cdot}0$, $\lambda_2 = 10$, $\lambda_3 = 0$, $\gamma_1 = 0{\cdot}2$: (a) electric potentials: a, 0·17; c, 0·5; e, 0·83; (b) pressure values γ: a = −1·5; b = −3·5; c = −5·5; d = −7·5; g = −13·5; j = −19·5; k = −21·5; l = −23·5; m = −25·5

The results for the first two sets of values are shown in Figures 8 and 9. The maximum velocities for the two cases are 2·477 and 1·883 respectively. The global velocity fields are not significantly different and are not shown. However, the pressure field has some noticeable variations from the previous cases as seen in the figures. We remark that previous attempts by others to compute a converged solution to the second set were unsuccessful.[11] The final set (1, −1) did not yield a convergent solution. Baleo *et al.*[3] were also unsuccessful in obtaining convergence for this case.

Finally we consider the same contraction–expansion flow in the presence of an applied electric field between the plates. The potential solution is shown in Figure 10(a). The velocity fields for suspension flow in all the cases considered were very close to the solution in the absence of the applied field and therefore will not be shown. There are some mild changes apparent in the pressure field in Figure 10(b)

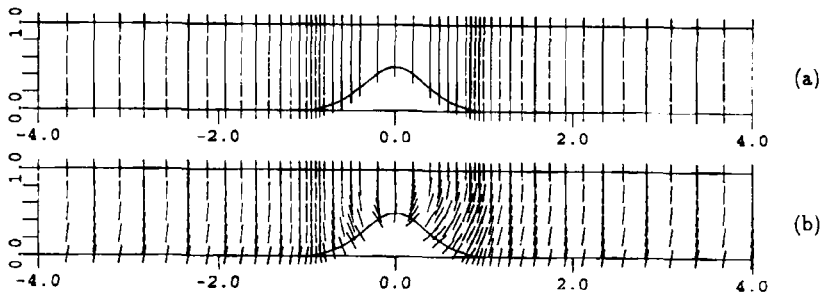

Figure 11. $G_1 = 0$, $\mu_2 = 0{\cdot}1$, $\mu_3 = -0{\cdot}05$, $\lambda_1 = 1{\cdot}0$, $\lambda_2 = 10$, $\lambda_3 = 0$, $\gamma_1 = 0{\cdot}2$: (a) initial director orientation; (b) director orientation at $t = 145$

and of course the director field is again significantly influenced as seen in the results of Figure 11 at $t = 145$ s (essentially steady state) for computation with time step $\Delta t = 0{\cdot}1$.

ACKNOWLEDGEMENT

This research was supported in part by a grant from Dowell Schlumberger.

APPENDIX I: ELECTRIC STRESS FROM VARIATIONAL PRINCIPLE

The electrical contribution to the stress tensor can also be obtained from a variational procedure. This approach reveals what choices of model coefficients are acceptable. From (7) the potential energy per unit volume for a dipole oriented in the direction of the anisotropic axis $\mathbf{n}$ can be determined by integrating the torque through the angle from $\mathbf{E}$ to $\mathbf{n}$ to yield

$$U = -cm^*(\mathbf{E}\cdot\mathbf{n}) - \frac{c}{2}\Delta\alpha(\mathbf{E}\cdot\mathbf{n})^2. \tag{47}$$

The potential energy change ΔU and the electric stress $\boldsymbol{\tau}^e$ are related by

$$\Delta U = \varepsilon_{ij}\tau^e_{ij}, \tag{48}$$

where ε_{ij} is a virtual deformation field in the sense that a vector $\mathbf{r}$ embedded in the continuum changes to $(\mathbf{I} + \boldsymbol{\epsilon})\cdot\mathbf{r}$ after the deformation. When ε_{ij} is small, the potential energy change can be approximated by

$$\Delta U = \delta\mathbf{n}\cdot\frac{\partial U}{\partial \mathbf{n}}, \tag{49}$$

where

$$\delta\mathbf{n} = \boldsymbol{\epsilon}\cdot\mathbf{n}. \tag{50}$$

Now

$$\begin{aligned}\frac{\partial U}{\partial \mathbf{n}} &= -cm^*\left(\mathbf{E}\cdot\frac{\partial \mathbf{n}}{\partial \mathbf{n}}\right) - c\Delta\alpha(\mathbf{E}\cdot\mathbf{n})\left(\mathbf{E}\cdot\frac{\partial \mathbf{n}}{\partial \mathbf{n}}\right)\\ &= -c[m^* + \Delta\alpha(\mathbf{E}\cdot\mathbf{n})](\mathbf{E}\cdot\mathbf{I}_{|\mathbf{n}|=1})\\ &= -m[(\mathbf{I}-\mathbf{nn})\cdot\mathbf{E}],\end{aligned} \tag{51}$$

where we have used $\partial \mathbf{n}/\partial \mathbf{n} = \mathbf{I} - \mathbf{nn} = \mathbf{I}_{|\mathbf{n}|=1}$. From (49) and (51) we see that

$$\Delta U = (\boldsymbol{\epsilon}\cdot\mathbf{n})\cdot m[(\mathbf{E}\cdot\mathbf{n})\mathbf{n} - \mathbf{E}] = \varepsilon_{ij} m[(\mathbf{E}\cdot\mathbf{n})n_i - E_i]n_j. \tag{52}$$

Comparing (52) with (48),

$$\tau^e_{ij} = m[(\mathbf{E}\cdot\mathbf{n})n_i n_j - E_i E_j] \tag{53}$$

or

$$\boldsymbol{\tau}^e = \lambda_2\gamma_1[(\mathbf{E}\cdot\mathbf{n})^2\mathbf{nn} - \mathbf{EE}\cdot\mathbf{nn}] + \lambda_3\gamma_1[(\mathbf{E}\cdot\mathbf{n})\mathbf{nn} - \mathbf{En}]. \tag{54}$$

Finally, comparing (54) with (14), we find that $\alpha_3 = 0$. When there is no electric field, one usually chooses α_3 to be a small negative number to ensure director anchoring instead of director tumbling.[2,21] In the presence of an electric field the anchoring is enhanced by the electric field. When $\alpha_3 = 0$, we see that $\lambda_1 = 1$, $\mu_4 = m$, $\mu_5 = -m$, $\mu_6 = 0$ and (15) becomes

$$\begin{aligned}\boldsymbol{\tau} =& 2\mu\mathbf{D} + [G_1 + \mu_2(\mathbf{n}\cdot\mathbf{D}\cdot\mathbf{n})]\mathbf{nn} + 2\mu_3[\mathbf{n}(\mathbf{D}\cdot\mathbf{n}) + (\mathbf{D}\cdot\mathbf{n})\mathbf{n}] \\ &+ \lambda_2\gamma_1[(\mathbf{E}\cdot\mathbf{n})^2\mathbf{nn} - \mathbf{EE}\cdot\mathbf{nn}] + \lambda_3\gamma_1[(\mathbf{E}\cdot\mathbf{n})\mathbf{nn} - \mathbf{En}],\end{aligned} \tag{55}$$

which is the form stated in (19).

APPENDIX II: ANALYTICAL SOLUTION FOR FLOW BETWEEN PARALLEL PLATES

In a two-dimensional, fully developed flow between parallel plates we assume that the velocity components $\mathbf{u} = (u, v, w)$ can be written as[2]

$$u = g(y), \qquad v = w = 0 \tag{56}$$

and we assume that the director angle β is constant with

$$\mathbf{n} = (n_x, n_y) = (\cos\ \beta, \sin\ \beta). \tag{57}$$

In the absence of the electric field, equation (13) can be reduced to

$$\begin{aligned}\frac{\partial n_x}{\partial t} &= \tfrac{1}{2}g'\ \sin\ \beta(1 + \lambda_1 - 2\lambda_1\ \cos^2\ \beta) = \tfrac{1}{2}g'\ \sin\ \beta[1 - \lambda_1\ \cos(2\beta)], \\ \frac{\partial n_y}{\partial t} &= \tfrac{1}{2}g'\ \cos\ \beta(-1 + \lambda_1 - 2\lambda_1\ \sin^2\ \beta) = -\tfrac{1}{2}g'\ \cos\ \beta[1 - \lambda_1\ \cos(2\beta)].\end{aligned} \tag{58}$$

We see that if $|\lambda_1| < 1$, there is no steady state solution (since $|\cos(2\beta)| \leq 1$). When $\lambda_1 \geq 1$, the steady state solution gives $\lambda_1\ \cos(2\beta) = 1$ or

$$\beta = \pm\tan^{-1}\left[\sqrt{\left(\frac{\lambda_1 - 1}{\lambda_1 + 1}\right)}\right], \tag{59}$$

which is equation (46).

Finally, the equation of motion and boundary conditions are satisfied by

$$p = p_0 - \frac{\Delta p}{l}x + g'\ \sin\ \beta\ \cos\ \beta(2\mu_3 + \mu_2\ \sin^2\ \beta), \tag{6}$$

$$g(y) = \frac{2yh - y^2}{2(\mu + \mu_3 + \mu_2\ \sin^2\ \beta\ \cos^2\ \beta)}\ \frac{\Delta p}{l}, \tag{61}$$

where $\Delta p/l$ is the pressure drop per unit length, p_0 is an arbitrary constant and h is the distance between the wall and the line of symmetry ($h = 1$ in our study).

REFERENCES

1. F. Gadala-Maria and A. Acrivos, 'Shear-induced structure in a concentrated suspension of solid spheres,' *J. Rheol.*, **24**, 799–814 (1980).
2. F. M. Leslie, 'Hamel flow of certain anisotropic fluids', *J. Fluid Mech.*, **18**, 595–601 (1964).
3. J. N. Baleo, M. Vincent and P. Navard, 'Finite element simulation of flow and director orientation of viscous anisotropic fluids in complex 2D geometries', *J. Rheol.*, **36**, 663–701 (1992).
4. J. D. Carlson, A. F. Sprecher and H. Conrad, eds. 'Electrorheological fluids', *Proc. 2nd Int. Conf. on ER Fluids*, Technomic, Lancaster, PA, 1990.
5. K. C. Wang, R. McLay and G. F. Carey, 'ER fluid modelling', in Carlson *et al.* (eds), *ER fluids*, Technomic, Lancaster, PA, 1990, pp. 41–52.
6. S. N. Shah, 'Rheological characterization of hydraulic fracturing slurries', *Paper SPE 22839*, 1991.
7. D. Hu, G. F. Carey and P. Majors, 'NMRI studies for non-Newtonian suspensions, CEOGRR report', *Tech. Rep.*, University of Texas at Austin, 1994.
8. F. M. Leslie, 'Theory of flow phenomena in liquid crystals', in G. H. Brown (ed.), *Advances in Liquid Crystals*, Vol. 4, Academic, New York, 1979, pp. 1–75.
9. D. M. Husband and F. Gadala-Maria, 'Anisotropic particle distribution in dilute suspensions of solid spheres in cylindrical Couette flow', *J. Rheol.*, **31**, 95–110 (1987).
10. P. G. de Gennes and J. Prost, *The Physics of Liquid Crystals*, 2nd edn, Oxford University Press, New York, 1993.
11. W. B. Vanderkeyden and G. Ryskin, 'Computer simulation of flow and molecular orientation in liquid crystal polymers', *J. Non-Newtonian Fluid Mech.*, **23**, 383–414 (1987).
12. M. Doi and S. F. Edwards, *The Theory of Polymer Dynamics*, Clarendon, Oxford, 1986.
13. M. Doi, 'Molecular dynamics and rheological properties of concentrated solutions of rodlike polymers in isotropic and liquid crystalline phases', *J. Polym. Sci., Polym. Phys. Ed.*, **19**, 229–243 (1981).
14. G. F. Carey and J. T Oden, *Finite Elements: Fluid Mechanics*, Prentice-Hall, Englewood Cliffs, NJ, 1986.
15. G. Ryskin, 'One modification of the Ericksen–Leslie equations in a two-dimensional motion', *J. Non-Newtonian Fluid Mech.*, **39**, 207–210 (1991).
16. S. Chandrasekhar, *Liquid Crystals*, 2nd edn, Cambridge University Press, Cambridge, 1992.
17. B. A. Finlayson, 'Numerical computations for the flow of liquid crystals', in J. F. Johnson and R. S. Porter (eds), *Liquid Crystals and Ordered Fluids*, Vol. 2, Plenum, New York, 1974, pp. 211–223.
18. H. C. Tseng, D. L. Silver and B. A. Finlayson, 'Application of the continuum theory of nematic liquid crystals', *Phys. Fluids*, **15**, 1213–1222 (1972).
19. T. Carlsson, 'Theoretical investigation of the shear flow of nematic liquid crystals with the Leslie viscosity $\alpha_3 > 0$: hydrodynamic analogue of first order phase transitions', *Mol. Cryst. Liq. Cryst.*, **104**, 307–334 (1984).
20. A. D. Rey and M. M. Denn, 'Converging flow of tumbling nematic liquid crystals', *Liq. Cryst.*, **4**, 253–272 (1989).
21. F. M. Leslie, 'Some constitutive equations for anisotropic fluids', *Q. J. Mech. Appl. Math.*, **19**, 357–370 (1966).